Journal of Physics: Conference Series **456** (2013) 012028 doi:10.1088/1742-6596/456/1/012028

Theory for optical Hall conductivity in the trilayer graphene in the quantum Hall regime

Takahiro Morimoto
Condensed Matter Theory Laboratory, RIKEN, Saitama, 351-0198, Japan

Mikito Koshino
Department of Physics, Tohoku University, Sendai, 980-8578, Japan

Hideo Aoki
Department of Physics, University of Tokyo, Hongo, Tokyo 113-0033, Japan

E-mail: tmorimoto@riken.jp

Abstract. We theoretically study optical Hall conductivities for ABA and ABC trilayer graphenes. In ABA-stacked trilayer, the resonance spectrum is shown to be a superposition of effective monolayer and bilayer contributions with band gaps, while ABC trilayer exhibits a distinct spectrum peculiar to the cubic-dispersed bands with a strong trigonal warping, where we found the signals associated with low-energy Dirac cones are conspicuous enough to be directly observable owing to a large Lifshitz-transition energy (~ 10 meV). We have also revealed how the presence or absence of the inversion symmetry affects the optical Hall conductivities.

1. Introduction

While the observation of the anomalous quantization of the static quantum Hall effect in graphene has established the existence of massless Dirac-quasiparticle in graphene [1, 2], physics of the optical (ac) Hall effect has only begun. The *optical Hall* conductivity $\sigma_{xy}(\omega)$ is an ac-extension of the static Hall conductivity, which has theoretically been proposed to be an interesting dynamical property to look at in the quantum Hall regime [3]. Experimentally, the optical Hall conductivity is measurable through Faraday rotation, since Faraday rotation angle is proportional to $\sigma_{xy}(\omega)$, where the angle is of the order of the fine-structure constant in the quantum Hall regime, as subsequently detected in a two-dimensional electron gas [4]. For graphene, giant cyclotron resonances in Faraday rotation is observed in the quantum Hall regime [5].

In the graphene physics, on the other hand, there are growing interests toward multilayer graphene, whose electronic structures are distinct from that of monolayer graphene. Especially, trilayer graphenes show various electronic structures according to the stacking order, where an ABA stacked trilayer has a monolayer-like linearly dispersed band plus a bilayer-like pair of parabolic bands, while an ABC stacking has a pair of cubic-dispersed bands. While the optical longitudinal conductivity $\sigma_{xx}(\omega)$ is mainly discussed so far, the the optical Hall conductivity

$\sigma_{xy}(\omega)$ has not been fully studied for multi-layer graphene in the quantum Hall regime. We have previously studied the optical Hall conductivities in trilayer graphene [6].

In the present paper, we discuss how the presence or absence of the inversion symmetry affects the optical Hall conductivities. It is argued that, when both the inversion symmetry and the time reversal symmetry are respected, the gaplessness of the bands are topologically protected in the graphene systems [7].

For ABA trilayer, we show the optical responses basically comes from Dirac contribution and bilayer contribution, which are both massive due to the lack of the inversion symmetry. The inversion symmetry is retained in ABC trilayer, so that the bands are gapless and zero energy LLs appear consequently.[8] We also show for ABC trilayer that the Lifshitz transition due to the trigonal warping affects the optical responses, where even away from the Lifshitz transition the trigonal warping effect manifest itself as satellite resonances.

2. ABA-stacked trilayer

For ABA stacked trilayer, the effective Hamiltonian around K_+/K_- points is given by a 6×6 matrix (the dimension being 2 sublattices $\times$ 3 layers) as [9, 10, 11, 12]

$$H_{\rm ABA} = \begin{pmatrix} 0 & v\pi^\dagger & 0 & v_3\pi & \gamma_2/2 & 0 \\ v\pi & \Delta' & \gamma_1 & 0 & 0 & \gamma_5/2 \\ 0 & \gamma_1 & \Delta' & v\pi^\dagger & 0 & \gamma_1 \\ v_3\pi^\dagger & 0 & v\pi & 0 & v_3\pi^\dagger & 0 \\ \gamma_2/2 & 0 & 0 & v_3\pi & 0 & v\pi^\dagger \\ 0 & \gamma_5/2 & \gamma_1 & 0 & v\pi & \Delta' \end{pmatrix}, \tag{1}$$

where $\pi = \xi\pi_x + i\pi_y$, $\pi^\dagger = \xi\pi_x - i\pi_y$, $\pi = \mathbf{p} + e\mathbf{A}$, with $\mathbf{A}$ being the vector potential arising from the applied magnetic field, and the valley index $\xi = \pm 1$ for $K_\pm$ points. The coefficient $v = \sqrt{3}a\gamma_0/(2\hbar)$ is the band velocity for monolayer graphene, $a \approx 0.246$ nm the distance between the nearest A sites, and $v_3 = \sqrt{3}a\gamma_3/(2\hbar)$ a velocity related to γ_3 that causes the trigonal warping. Δ' is the on-site energy difference between the atoms with and without vertical bond γ_1, and $\gamma_2(\gamma_5)$ are the next-nearest interlayer hoppings between $A1$ and $A3$ ($B1$ and $B3$). We adopt the values for bulk graphite: γ_0=3.2eV, γ_1=0.39eV, γ_3=0.32eV, γ_2=-0.020eV, γ_5=0.038eV, and Δ'=0.050eV. [13, 14] There is another interlayer hopping parameters, γ_4, connecting A1 (B1) and A2 (B2), which introduces a small electron-hole asymmetry to the band structure and we do not consider in this paper.

With a unitary transformation [12, 15, 16, 17, 18], this Hamiltonian is decomposed into two blocks corresponding to a 2×2 massive Dirac Hamiltonian with a shift in Fermi energy and a 4×4 gapped bilayer Hamiltonian with another energy shift. So the low-energy physics of ABA trilayer amounts to a superposition of gapped monolayer and gapped bilayer band contributions as seen in the low-energy band structure (Fig.1(a)).

In Fig.1(b), LLs are plotted against magnetic field B, which are labeled with M (B) for monolayer (bilayer) blocks, Landau index n, and band index $\pm$ (for $n \geq 1$). For moderate magnetic fields $B \sim 1$ T, the Landau level spacing $\propto \sqrt{B}$ for monolayer is much larger than that for bilayer $\propto B$. ABA trilayer lacks an inversion center and bands are gapped. As a consequence, zero-energy LLs of monolayer and bilayer appear at the bottom (top) of the conduction (valence) bands for K_+ (K_-) valley.

Now let us move on to the optical Hall conductivity ($\sigma_{xy}(\omega)$), which is evaluated from the Kubo formula as

$$\sigma_{\alpha\beta}(\omega) = \frac{\hbar}{iL^2}\sum_{ab} j_\alpha^{ab} j_\beta^{ba} \frac{f(\epsilon_b) - f(\epsilon_a)}{\epsilon_b - \epsilon_a} \frac{1}{\epsilon_b - \epsilon_a - \hbar\omega - i\eta}, \tag{2}$$

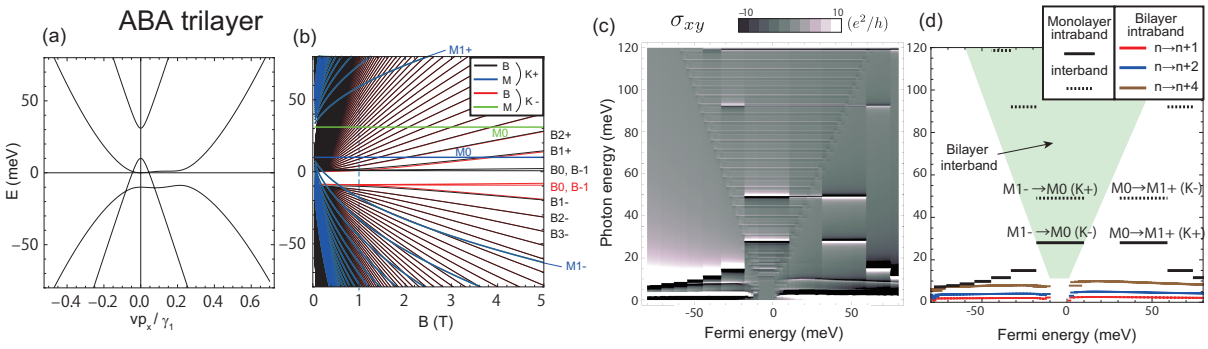

Figure 1. (a) Band structure and (b) Landau levels against magnetic field for ABA-stacked trilayer graphene. (c) Optical Hall $\sigma_{xy}(\epsilon_F, \omega)$ grey-scale plotted against the Fermi energy ϵ_F and the frequency ω for a magnetic field $B = 1T$ (a dashed line in (b)). (d) A diagram indicating allowed resonances in σ_{xy}.

where $f(\varepsilon)$ is the Fermi distribution, ϵ_a the energy of the eigenstate $|a\rangle$, $\mathbf{j}^{ab} = \langle a|\mathbf{j}|b\rangle$ the matrix element of the current operator $\mathbf{j} = \partial H/\partial \mathbf{A}$, and η a small energy cutoff for a stability of the calculation[3]. In order to show the resonance structures in optical responses clear, we set to $\eta = 0.15$ meV, which is a small value compared to realisitic situations. Larger η makes the resonances more broadened, while it does not alter their qualitative behaviors.

The result for the optical Hall conductivity $\sigma_{xy}(\epsilon_F, \omega)$ is plotted against the Fermi energy ϵ_F and frequency ω for ABA stacked trilayer graphene QHE system in Fig.1(c). We can discern contributions from monolayer-like Dirac LLs and those from bilayer LLs, both of which exhibit intra-band and inter-band transitions. Since Dirac cone is massive due to a breaking of an inversion symmetry and M0 LL is situated at the bottom of conduction band for K_+ valley and the top of valence band for K_-, $M0 \to M1+$ resonance occurs at a lower energy than $M1- \to M0$ for K_+, and vice versa for K_- valley. A cancellation of resonances in σ_{xy}, due to opposite signs in current matrices, occurs between $M1- \to M0$ for K_+ and $M0 \to M1+$ for K_- for a region of Fermi energy between $M0(K_+)$ and $M0(K_-)$, while this is not the case with σ_{xx}. For bilayer contributions satellites appear due to the trigonal warping from the transitions $(n, s) \leftrightarrow (n+1+3m, s')$ and $(n, s) \leftrightarrow (n+2+3m, s')$, since the trigonal warping due to γ_3 term mixes (n, s) and $(n + 3m, s')$.

The resonance frequency for intra-band transition within the conduction band is larger than those within the valence band, which is a consequence of an electron-hole *a*symmetry in the bilayer bands. Different cyclotron masses for electron and hole bands prevent a complete cancellation between $(n, -) \to (n + 1, +)$ and $(n + 1, -) \to (n, +)$ transitions, which results in small interband transitions in a wide region of Fermi energy.

3. ABC-stacked trilayer

If we turn to ABC stacked bilayer graphene, the effective Hamiltonian around K point is a 6×6 matrix as [9, 19, 20]

$$H_{\rm ABC} = \begin{pmatrix} 0 & v\pi^\dagger & 0 & v_3\pi & 0 & \gamma_2/2 \\ v\pi & 0 & \gamma_1 & 0 & 0 & 0 \\ 0 & \gamma_1 & 0 & v\pi^\dagger & 0 & v_3\pi \\ v_3\pi^\dagger & 0 & v\pi & 0 & \gamma_1 & 0 \\ 0 & 0 & 0 & \gamma_1 & 0 & v\pi^\dagger \\ \gamma_2/2 & 0 & v_3\pi^\dagger & 0 & v\pi & 0 \end{pmatrix}. \tag{3}$$

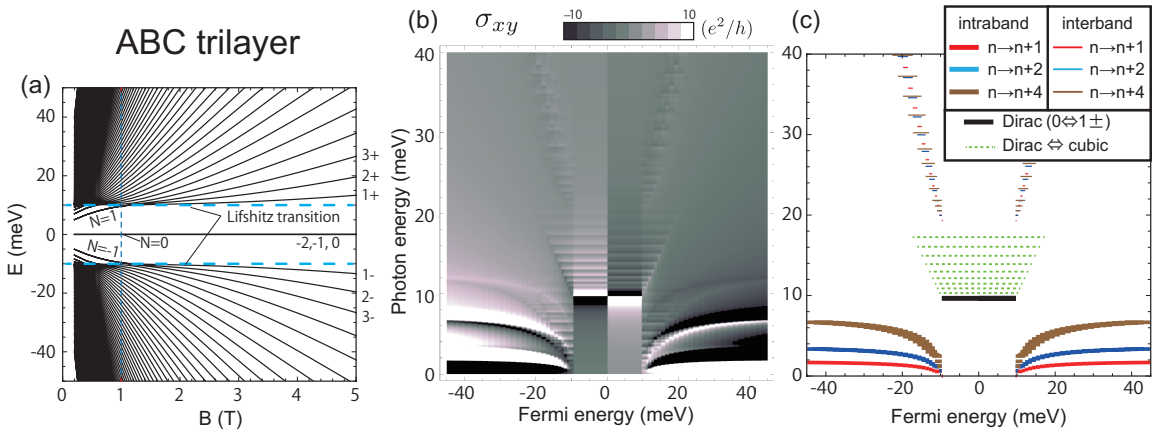

Figure 2. (a) Landau levels against magnetic field for ABC-stacked trilayer graphene. (b) Optical Hall $\sigma_{xy}(\epsilon_F, \omega)$ grey-scale plotted against the Fermi energy ϵ_F and the frequency ω for a magnetic field $B = 1T$ (a dashed line in (a)). (c) A diagram indicating allowed resonances in σ_{xy}.

We can derive a low-energy effective Hamiltonian as a 2×2 matrix with basis for A1 and B3, where we eliminate the states coupled by γ_1. As in the case of bilayer, a perturbation in ε/γ_1 gives the effective Hamiltonian for ABC trilayer graphene as [20],

$$H_{\rm ABC}^{\rm (eff)} = \frac{v^3}{\gamma_1^2}\begin{pmatrix} 0 & (\pi^\dagger)^3 \\ \pi^3 & 0 \end{pmatrix} + \left(\frac{\gamma_2}{2} - \frac{2vv_3\pi^2}{\gamma_1}\right)\begin{pmatrix} 0 & 1 \\ 1 & 0 \end{pmatrix}, \tag{4}$$

where $\pi^2 = (\pi^\dagger\pi + \pi\pi^\dagger)/2$. In zero magnetic field, the first term gives a pair of cubic-dispersed bands touching at zero energy, while the second term involving γ_2 and v_3 causes a trigonal warping in the band dispersion. In a low-energy region, the cubic bands are reformed into three Dirac cones at off-center momenta located in 120° symmetry around $K_\pm$ point. The Lifshitz transition occurs at $E_{\rm Lifshitz} \approx \frac{\gamma_2}{2} \sim 10\,{\rm meV}$, which is an order of magnitude *greater* than in bilayer's.

If we first neglect γ_2 and v_3 to consider the cubic part alone in Eqn. 4, LLs are[9, 20]

$$\varepsilon_{n,s} = s\hbar\omega_{\rm ABC}\sqrt{n(n+1)(n+2)}, \tag{5}$$

where $n \geq -2$ is the Landau index, $s = \pm$ (only for $n \geq 1$) the band index, and $\hbar\omega_{\rm ABC} = \frac{v^3}{\gamma_1^2}(2\hbar eB)^{\frac{3}{2}}$. A peculiar magnetic field dependence of cyclotron energy $\propto B^{\frac{3}{2}}$ for ABC trilayer graphene implies a smaller LL spacing as compared with the monolayer's LL $\propto B^{\frac{1}{2}}$ and bilayer's LL $\propto B$ for weak magnetic fields.

The trigonal warping due to γ_2 and v_3 hybridizes $\psi_{n,s}$ with $\psi_{n+3m,s'}$. In the low-energy region $|E| < E_{\rm Lifshitz}$, the spectrum is reconstructed into the monolayer-like Landau levels from small Dirac cones as a series $\varepsilon_N = {\rm sgn}(N)\sqrt{N}\hbar\omega_{\rm trig}$, with $\hbar\omega_{\rm trig} \simeq 10\sqrt{\frac{B}{1{\rm T}}}$ meV.

Now we go back to the original 6×6 Hamiltonian (Eqn.3) to discuss the optical Hall conductivity calculated with diagonalization and Kubo formula. In the LL spectrum in Fig.2(a), a Lifshitz transition is clearly identified at $E_{\rm Lifshitz} = 10$meV, which separates Dirac LLs and ABC cubic LLs. Since the inversion symmetry is *preserved* in ABC trilayer so that the band cannot be gapped, 3 zero-energy LLs appear which correspond to 3 gapless Dirac cones within the Lifshitz transition energy.

Figure 2(b) shows the optical Hall conductivities $\sigma_{xy}(\epsilon_F, \omega)$ plotted against the Fermi energy ϵ_F and frequency ω for ABC stacked trilayer graphene QHE system with $B = 1$T. At this magnetic field, there are three Landau levels $n = -1, 0, 1$ in each Dirac cone, where the $n = \pm 1$ levels are close to the Lifshitz transision. The higher levels are outside the Dirac cones, and can be regarded to belong to the the cubic dispersion. Accordingly we see cyclotron resonances between $1- \to 0$ and $0 \to 1+$ in $E_F < E_{\rm Lifshitz}$, while outside we see transitions between cubic LLs $\propto B^{\frac{3}{2}}$ with much smaller level spacings than for Dirac LLs $\propto \sqrt{B}$. In addition to resonances $n \leftrightarrow n+1$, the trigonal warping again gives rise to satellite transitions, $n \leftrightarrow n+4$ and $n \leftrightarrow n+2$, with opposite resonance weights. There also emerge small resonances between Dirac $n = 0$ LL and cubic LLs across the Lifshitz transition energy. Due to the ABC trilayer LLs arising from the cubic dispersion (Eqn.5) the intra-band transition energies show behaviors $\propto n^{1/2}$ against the Landau index n, which is different from monolayer ($\propto n^{-1/2}$) or bilayer (constant), while the inter-band transition energies are qualitatively similar to $\sim 2\epsilon_F$.

4. Summary

We have studied the optical Hall conductivities for ABA and ABC trilayer graphenes. The ac optical responses in the ABA-stacked trilayer graphene accommodates a mixture of contributions from an effective massive monolayer and from an effective gapped bilayer with the trigonal warping effect. In the case of ABC trilayer graphene the trigonal warping effect is an order of magnitude enhanced than in bilayer graphene, so it will be experimentally more feasible to access the effects induced by the trigonal warping. We have discussed how the differences between ABA and ABC trilayers are related to the absence or presence of the inversion symmetry.

HA acknowledges the financial support by Grants-in-Aid for Scientific Research No.23340112 from JSPS, while MK the Grants-in-Aid for Scientific Research No.24740193 from JSPS, and by JST-EPSRC Japan-UK Cooperative Programme Grant No. EP/H025804/1.

References

[1] Novoselov K, Geim A, Morozov S, Jiang D, Katsnelson M, Grigorieva I, Dubonos S and Firsov A 2005 *Nature* **438** 197–200
[2] Zhang Y, Tan Y W, Stormer H L and Kim P 2005 **438** 201
[3] Morimoto T, Hatsugai Y and Aoki H 2009 *Phys. Rev. Lett.* **103** 116803
[4] Ikebe Y, Morimoto T, Masutomi R, Okamoto T, Aoki H and Shimano R 2010 *Phys. Rev. Lett.* **104** 256802
[5] Crassee I, Levallois J, Walter A, Ostler M, Bostwick A, Rotenberg E, Seyller T, Van Der Marel D and Kuzmenko A 2011 *Nature Physics* **7** 48–51
[6] Morimoto T, Koshino M and Aoki H 2012 *Phys. Rev. B* **86**(15) 155426
[7] Mañes J L, Guinea F and Vozmediano M A H 2007 *Phys. Rev. B* **75**(15) 155424
[8] Koshino M and McCann E 2010 *Phys. Rev. B* **81**(11) 115315
[9] Guinea F, Castro Neto A H and Peres N M R 2006 *Phys. Rev. B* **73**(24) 245426
[10] Partoens B and Peeters F 2006 *Physical Review B* **74** 075404
[11] Lu C, Chang C, Huang Y, Chen R and Lin M 2006 *Physical Review B* **73** 144427
[12] Koshino M and Ando T 2007 *Phys. Rev. B* **76**(8) 085425
[13] Charlier J, Gonze X and Michenaud J 1991 *Phys. Rev. B* **43** 4579
[14] Dresselhaus M and Dresselhaus G 2002 *Advances in Physics* **51** 1–186
[15] Koshino M and Ando T 2008 *Phys. Rev. B* **77**(11) 115313
[16] Koshino M and McCann E 2009 *Phys. Rev. B* **79** 125443
[17] Koshino M and Ando T 2009 *Solid State Communications* **149** 1123–1127
[18] Koshino M and McCann E 2011 *Phys. Rev. B* **83**(16) 165443
[19] Lu C L, Lin H C, Hwang C C, Wang J, Lin M F and Chang C P 2006 *Appl. Phys. Lett.* **89** 221910
[20] Koshino M and McCann E 2009 *Phys. Rev. B* **80** 165409